

LA-4369-TR

4.3

CIC-14 REPORT COLLECTION  
REPRODUCTION  
COPY

LOS ALAMOS SCIENTIFIC LABORATORY  
of the  
University of California  
LOS ALAMOS • NEW MEXICO

Angular Anisotropy and Structure  
of the Fission Barrier

LOS ALAMOS NATIONAL LABORATORY



3 9338 00377 8353

UNITED STATES  
ATOMIC ENERGY COMMISSION  
CONTRACT W-7405-ENG-36

## LEGAL NOTICE

This report was prepared as an account of Government sponsored work. Neither the United States, nor the Commission, nor any person acting on behalf of the Commission:

A. Makes any warranty or representation, expressed or implied, with respect to the accuracy, completeness, or usefulness of the information contained in this report, or that the use of any information, apparatus, method, or process disclosed in this report may not infringe privately owned rights; or

B. Assumes any liabilities with respect to the use of, or for damages resulting from the use of any information, apparatus, method, or process disclosed in this report.

As used in the above, "person acting on behalf of the Commission" includes any employee or contractor of the Commission, or employee of such contractor, to the extent that such employee or contractor of the Commission, or employee of such contractor prepares, disseminates, or provides access to, any information pursuant to his employment or contract with the Commission, or his employment with such contractor.

This translation has been prepared in response to a specific request; It is being given standard distribution because of its relevance to the nuclear energy program. Reasonable effort has been made to ensure accuracy but no guarantee is offered.

Printed in the United States of America. Available from  
Clearinghouse for Federal Scientific and Technical Information  
National Bureau of Standards, U. S. Department of Commerce  
Springfield, Virginia 22151

Price: Printed Copy \$3.00; Microfiche \$0.65

**LOS ALAMOS SCIENTIFIC LABORATORY**  
of the  
**University of California**  
LOS ALAMOS • NEW MEXICO

**Angular Anisotropy and Structure  
of the Fission Barrier**

by

**K. D. Androsenko, S. B. Ermagambetov,  
A. V. Ignatiuk, N. S. Rabotnov,  
G. N. Smirenkin, A. S. Soldatov,  
L. N. Usachev, and D. L. Shpak,**  
Institute of Physics and Energetics, Obninsk, USSR;

**S. P. Kapitsa, and Iu. M. Tsipeniuk,**  
Institute for Physical Problems, Moscow, USSR;

**I. Kovach,**  
Central Institute for Physical Research, Budapest, Hungary

Source: Institute of Physics and Energetics, FEI-185, 1969.

Translated by

Helen J. Dahlby



## ANGULAR ANISOTROPY AND STRUCTURE OF THE FISSION BARRIER

by

K. D. Androsenko, S. B. Ermagambetov, A. V. Ignatiuk, N. S. Rabotnov,  
G. N. Smirenkin, A. S. Soldatov, L. N. Usachev, D. L. Shpak,  
S. P. Kapitsa, Iu. M. Tsipeniuk, and I. Kovach

### ABSTRACT

Measurements of the angular distributions of fragments from fission by neutrons of the target nuclei of  $^{232}\text{Th}$ ,  $^{238}\text{U}$ ,  $^{237}\text{Np}$ ,  $^{238}\text{Pu}$ ,  $^{240}\text{Pu}$ ,  $^{242}\text{Pu}$ , and  $^{241}\text{Am}$  and by photons of  $^{232}\text{Th}$ ,  $^{238}\text{U}$ ,  $^{238}\text{Pu}$ ,  $^{240}\text{Pu}$ , and  $^{242}\text{Pu}$  are reported. Investigations of the  $(n, f)$  reaction were carried out on the electrostatic generators of the Institute of Physics and Energetics, and investigations of photofission, on a microtron of the Institute of Physical Problems of the Academy of Sciences of the USSR, at 12 MeV. Most attention was paid to study of the near-threshold region of excitation energies. The data obtained do not fit the traditional description of fission probability, but are satisfactorily explained by the two-hump barrier concept. Questions about the quasi-stationary nuclear states in the second well, the structure of the barriers, the even-odd differences of fission probability, and the energy gap of a nucleus with large deformations are discussed.

### INTRODUCTION

The angular anisotropy of the distribution of fission fragments results from the primary orientation of the angular momentum,  $\vec{T}$ , of the nucleus relative to the beam of bombarding particles and the nonuniform distribution of the projections of the momentum  $K$  on the axis of symmetry (direction of splitting). The observed spectrum,  $f(K)$ , depends on the energy of excitation into the transition state  $E^* = E - E_f$  and the method of excitation determining a practicable set of angular momenta. The region of low  $E^*$ , where the nucleus is cold and a few transition quantum states--fission channels--participate in fission<sup>1,2</sup> is of special interest. The appearance of a complex structure in the energy dependence of the angular distributions of the fragments,  $W(\theta)$ , near the threshold in the cross section,  $\sigma_f$ , is associated with discrete states in the spectrum of the lowest fission channels.

Studies of near-threshold fission of nuclei disclosed a number of qualitative effects attesting

to the fruitfulness of the concept of the fission-channel model. Study of even-even fissioning nuclei, an application in which the model using a fission-channel spectrum analogous to the spectra of excited equilibrium states leads to concrete results, is most important. The expected quantum structure of the barrier has been observed during study of photofission<sup>3</sup> and reactions of the  $(d, pf)$  type.<sup>4,5</sup>

However, more detailed experiments and a detailed quantitative analysis of the energy dependence of the angular anisotropy<sup>6-10</sup> showed the incompleteness of the traditional description of nuclear fission near the threshold.<sup>1,2</sup> Explanation of a number of properties and phenomena that do not fit the generally accepted N. Bohr-Wheeler-A. Bohr concept, among them angular anisotropy, became possible with reconsideration of the concepts of the shape of the fission barrier. In 1967 Strutinskii<sup>11</sup> calculated the potential energy of deformation of the nucleus, taking into account shell effects. His

calculations show the significant divergence of the shape of the fission barrier from the parabola motivated by the liquid-drop model. According to Strutinskii, the real fission barrier in the usual unidimensional representation is a curve with two maxima. The physical concepts of the new represen-

lem. Identification of the predominant fission channels  $K^\pi$  and reduction of the energy dependence of the penetrability of the barriers  $P_{K^\pi}(E_n)$  were accomplished, as usual, by empirical choice of those quantum characteristics that would ensure agreement of the calculation

$$\frac{d\sigma_f(\theta, E_n)}{d\Omega} \sim \frac{\lambda^2(E_n)}{4} \sum_{\tau, k, \pi} (2T+1) T_{\ell}^{\tau}(E_n) \frac{P_{k\pi}(E_n \cdot \gamma_{\tau k}) \cdot W_{\tau k}(\theta)}{\sum_{\ell, j', m} T_{\ell}^{j'}(E_n - E_m)} \quad (1)$$

tations of the barrier shape and the quasi-stationary states in the well between the maxima<sup>12,13</sup> are the basis of the so-called two-hump fission barrier model.

This paper investigates questions about the angular anisotropy and structure of the fission barrier. Some recent measurements with monoenergetic neutrons in electrostatic generators at the Institute of Physics and Energetics and with photons from bremsstrahlung in the microtron of the Institute of Physical Problems of the Academy of Sciences of the USSR are included. Most of the data were obtained by track technology. A detailed description of the experiments and their results will be given in another report. This report aims to demonstrate the inadequacy of the traditional description of angular anisotropy of fission and to discuss the possibility of refining it using the two-hump barrier model.

## I. EXPERIMENTAL RESULTS AND CONSEQUENCES

### A. Fission of $^{232}\text{Th}(n, f)$ near the Threshold

The results of measurements of the fission cross section,  $\sigma_f$ ,<sup>14</sup> and angular distributions of the fragments,  $W(\theta)$ , are given in Figs. 1 and 2. The curves in Fig. 2,  $W(\theta) = \sum_{r=0}^{\infty} \alpha_{2n} P_{2n}(\alpha\theta)$ , where  $P_{2n}(\alpha\theta)$  are Legendre polynomials, are calculated by the least-squares method. Data on the angular anisotropy  $W(0^\circ)/W(90^\circ)$  are shown in the insert to Fig. 1, where they are compared with the results of other measurements.<sup>8,15,16</sup> The angular distributions measured by different authors<sup>15,16</sup> agree less well than do the data on the angular anisotropy.

Obtaining detailed information on  $\sigma_f$  and  $\frac{d\sigma_f(\theta)}{d\Omega} \sim W(\theta)$  for a channel analysis was a prob-

lem. Identification of the predominant fission channels  $K^\pi$  and reduction of the energy dependence of the penetrability of the barriers  $P_{K^\pi}(E_n)$  were accomplished, as usual, by empirical choice of those quantum characteristics that would ensure agreement of the calculation with experiment. In Eq. (1) we neglected the fission  $\Gamma_f$  and radiation  $\Gamma_\gamma$  widths relative to the neutron width  $\Gamma_n \sim \sum_{\ell, j', m} T_{\ell}^{j'}(E_n - E_m)$ .  $\lambda$  is the wavelength of the neutron,  $T_{\ell}^{j'}$  are the optical coefficients of penetrability of the neutrons,<sup>17</sup> and  $\Pi = (-1)^\ell$ . The index  $m$  shows the levels of the target nucleus, and  $\gamma_{\tau k}$  takes into account the dependence of the penetrability of the fission barrier on the total angular momentum,  $T$ , in accordance with the usual assumption that the difference in  $P_{k\pi}$  for different  $T$  reduces to a subtraction of the energy of rotation  $E_{rot} = \frac{\lambda^2}{2F} [T(T+4) - K(K+4)]$  from the energy concentrated in the fission degrees of freedom (we assumed that  $\lambda^2/2F = 4$  keV).

The classical channel analysis scheme<sup>2</sup> consists in finding the height of the barrier  $E_f^{K^\pi}$  and the parameter of curvature  $hw_{K^\pi}$ , related to  $P_{K^\pi}(E_n)$  by the well-known Hill-Wheeler relation for a parabolic barrier,

$$P_{K^\pi}(E_n) = \left[ 1 + \exp \left( 2\pi \frac{E_f^{K^\pi} - E_n - B_k}{hw_{K^\pi}} \right) \right]^{-1}, \quad (2)$$

where  $B_n$  is the binding energy of the neutron.

Such calculations have been carried out for the reactions  $^{232}\text{Th}(n, f)$ <sup>16</sup> and  $^{234}\text{U}(n, f)$ ,<sup>18</sup> but they do not describe the shape of  $\sigma_f(E_n)$  in detail because Eq. (2) depends monotonically on  $E_n$  and ignores the resonance phenomena noted in Refs. 6 and 7. Our analysis was made using Vorotnikov's proposed method,<sup>6</sup> in which no limitations are imposed on the energy dependence of  $P_{K^\pi}(E_n)$ .

Note the more important results of the analysis.

1. For all  $E_n$ , we could obtain agreement of the calculation of  $W(\theta)$  with experiment within the

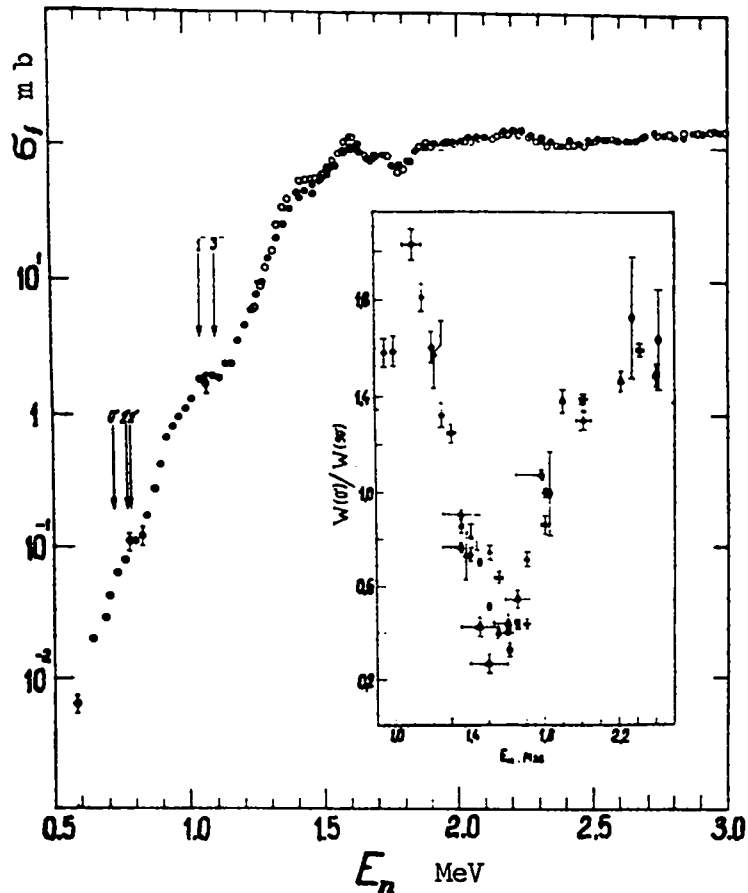


Fig. 1. Fission cross section of  $^{232}\text{Th}$  as a function of neutron energy  $E_n$ :  
 ● - Ref. 14, ○ - data from the Table of neutron cross sections  
 Insert: angular isotropy. ● - this paper, △ - Ref. 8, △, ◇ - Ref. 15.

limit of experimental error using only two or three combinations of the dominating states  $K^\pi$ . The main qualitative feature of the observed  $K^\pi$  spectrum is the abrupt change, in the narrow energy interval  $E_n \sim 0.1$  to  $0.2$  MeV, of the role of the individual states (introduction and disappearance), which attests to an irregular "resonance" behavior of  $P_{K^\pi}(E_n)$ , in disagreement with Wheeler.<sup>2</sup>

2. Ambiguity characterizes the identification of even the dominant fission channels. Determination of the parity of the  $K = \frac{1}{2}$  states, which make a significant contribution at all energies studied, was not successful; it is difficult to distinguish the states  $K^\pi = 3/2^+$  and  $5/2^-$  and  $5/2^+$  and  $7/2^-$ , respectively. Therefore, in Fig. 3 we show variations of the analytical results for

$K^\pi = \frac{1}{2}^+$  and  $\frac{1}{2}^-$ , and in each case in separate regions of  $E_n$  show the possible pairs of  $P_{K^\pi}$  that agree about equally with experiment, (broken and solid lines). The indefiniteness of the parameter  $\lambda^2/2F$  can also cause errors. However, the identification of  $K^\pi$  (but not the absolute value of  $P_{K^\pi}$ ) is insensitive to lack of detailed information about the levels of the target nucleus above 1.2 MeV.

3. The fact that the main result of the analysis--the presence of resonances of  $P_{K^\pi}(E_n)$  with a width of  $\sim 0.1$  MeV--is not affected by the indefinite identification of quantum characteristics of the channels is fortunate. The irregularities of  $\sigma_f(E_n)$  near 1.1 and 1.6 MeV are related to the resonances  $P_{\frac{1}{2}^\pi}$  and  $P_{\frac{3}{2}^\pi}$ , respectively; the traditional explanation by the competition of the neutron

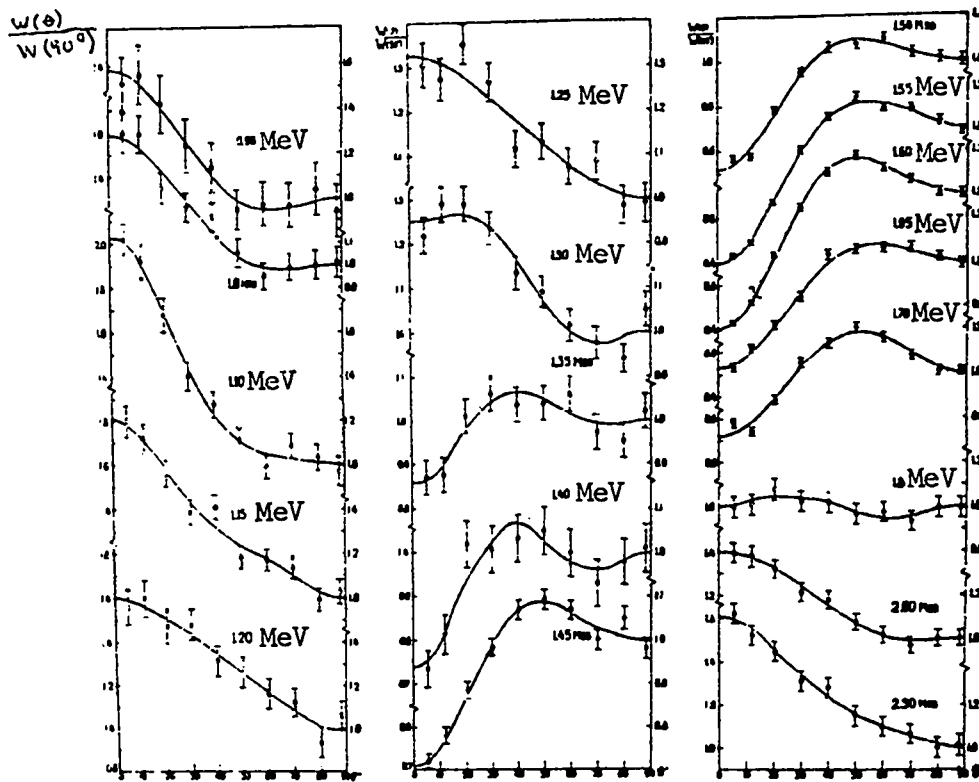


Fig. 2. Angular distributions of fragments of  $^{232}\text{Th}$  fission by neutrons.

width<sup>2</sup> is unsuitable in these cases. The value of  $P_{\frac{1}{2}\pi}(0)$  obtained by exponential extrapolation to  $E_n = 0$  diverges strongly from the penetrability calculated by the cross section of the fission of  $^{232}\text{Th}$  by thermal neutrons.<sup>19</sup> The latter exceeds the extrapolated value<sup>14</sup> by more than a factor of one thousand. This fact shows that the irregular change in the penetrability of the barrier is preserved in the deep subbarrier excitation region. A clearer picture of the resonance effects on  $P(E)$  is given by Gokhberg et al.<sup>20</sup>

B. Fission of  $^{238}\text{U}$ ,  $^{237}\text{Np}$ ,  $^{238}\text{Pu}$ ,  $^{240}\text{Pu}$ ,  $^{242}\text{Pu}$ , and  $^{241}\text{Am}$  by Neutrons

Measurement of the angular distributions of the fission fragments of  $^{238}\text{U}$ ,  $^{240}\text{Pu}$ , and  $^{242}\text{Pu}$  was mainly in the near-threshold region of neutron energies; for  $^{237}\text{Np}$ ,  $^{238}\text{Pu}$ , and  $^{241}\text{Am}$ , it was at the threshold of the  $(n, \text{nf})$  reaction. The coefficient of angular anisotropy  $A = W(0^\circ)/W(90^\circ) - 1$  for five target nuclei is shown in Fig. 4. For three of them,  $^{238}\text{Pu}$  ( $\approx 85\%$ ),  $^{240}\text{Pu}$  ( $\approx 93\%$ ), and  $^{242}\text{Pu}$  ( $\approx 95\%$ ), the measurement accuracy in the subthresh-

old region was limited by isotopic impurities.

A general property of the nuclei investigated is the almost total lack of channel effects in the angular distribution of fragments. The angular distributions for isotopes of neptunium, plutonium, and americium for all energies, including subthreshold, are well described by the simple expression

$$\frac{W(\theta)}{W(90^\circ)} = 1 + A \cos^2 \theta . \quad (3)$$

The conformity of the anisotropic part of  $W(\theta)$  to the quadratic dependence on  $\cos \theta$  for sufficient excitations is usually thought to indicate a statistical distribution of  $K$ ,<sup>27</sup>

$$f(K) \sim \exp - \left( \frac{K^2}{2K_0^2} \right) . \quad (4)$$

For a description of  $W(\theta)$ , in this case the relation of the statistical theory,

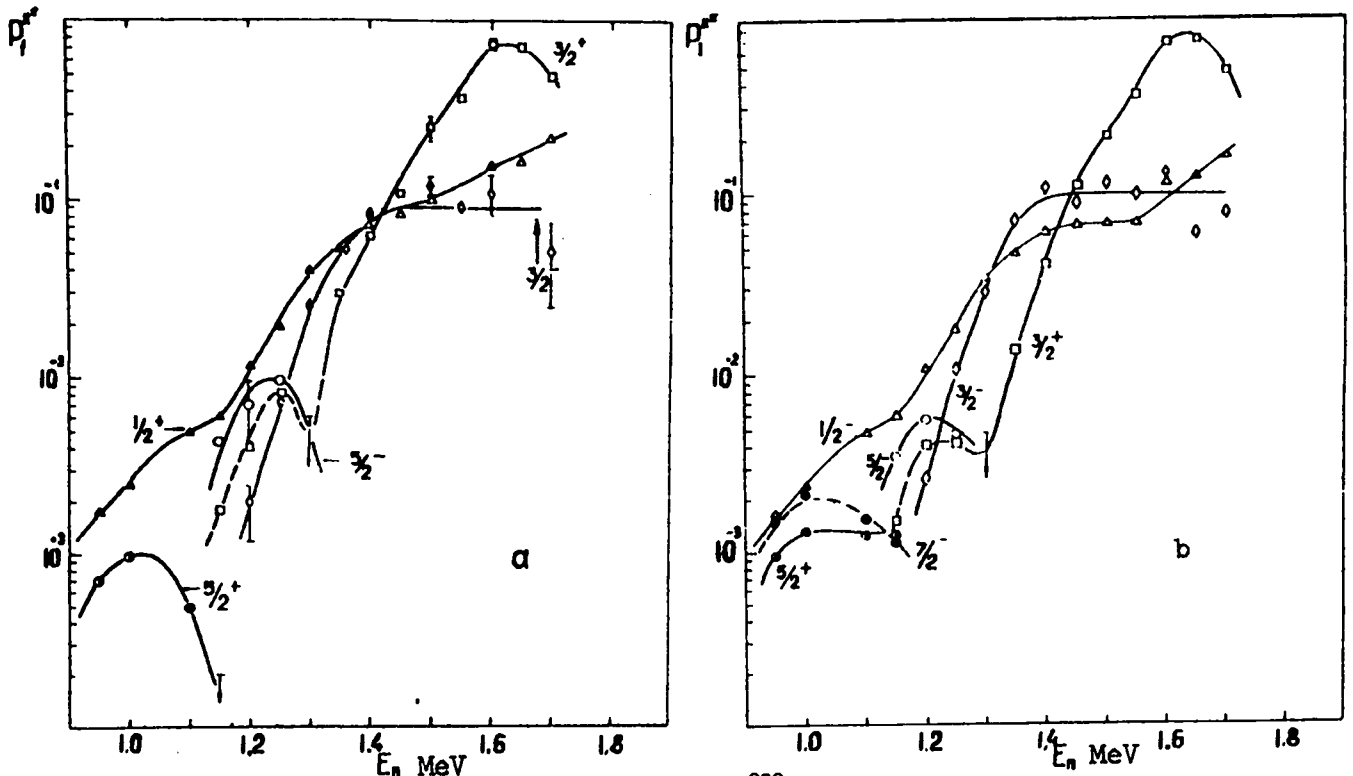


Fig. 3. Dependence of penetrability of fission barrier for  $^{232}\text{Th} (n, f)$  on neutron energy,  $E_n$ , for different quantum states of nucleus  $K^\pi$ , with the assumption that the parity of the channels  $K = 1/2$  is: a) positive, b) negative (see text).

$$W(\theta) \sim \text{Sin}^{-3} \theta \int_0^{P \text{Sin}^2 \theta} x^{\frac{1}{2}} e^{-x} \text{Io}(x) dx$$

$$= \text{Sin}^{-3} \theta \cdot \varphi(P \text{Sin}^2 \theta), \quad (5)$$

is widely used for small  $P = \frac{\langle T^2 \rangle}{2K_0^2}$ , i.e., a small anisotropy, which converts to Eq. (3). For the nuclei considered,  $A \lesssim 0.2$ .

Nonetheless, the conformity of the experimental data on  $W(\theta)$  to Eq. (3) in the  $(n, f)$  reaction cannot, without additional analysis, be considered an adequate indication of the distribution of Eq. (4). In fact, Eq. (3) is fulfilled with any spectrum of the channels for low energies,  $E_n \lesssim 0.5$  MeV, when waves with  $l \lesssim 1$  dominate the cross section of the formation of a compound nucleus. Only the contribution of higher angular momenta leads to deviations

from Eq. (3).

Let us satisfy ourselves from the example of  $^{238}\text{Pu} (n, f)$  that the experimental angular distributions of the fragments cannot be explained by enlisting a small number of  $K^\pi$  states. This reaction is also interesting in that a channel analysis carried out for it by Vorotnikov et al.<sup>24</sup> leads to a contradictory conclusion. According to Vorotnikov et al., the fission of  $^{238}\text{Pu}$  by neutrons has a threshold at  $E_n \approx 0.8$  to 1.0 MeV and proceeds to 1.5 MeV primarily through two types of  $K^\pi$  states,  $\frac{1}{2}^-$  and  $3/2^-$ . In Fig. 5 our experimental distributions are compared with a calculation made by the scheme used above in the analysis of the  $^{232}\text{Th} (n, f)$  reaction. Other simple combinations of  $K^\pi$  show still greater divergence from experiment.

A clear demonstration of the participation of many states in the fission of heavy nuclei near the threshold was obtained in a study of the  $^{238}\text{U} (n, f)$  reaction.<sup>9</sup> The coefficient of angular anisotropy agrees with Lamphere's data<sup>8</sup> and reaches 0.6. In this case Eq. (3) is not satisfactory, and to check



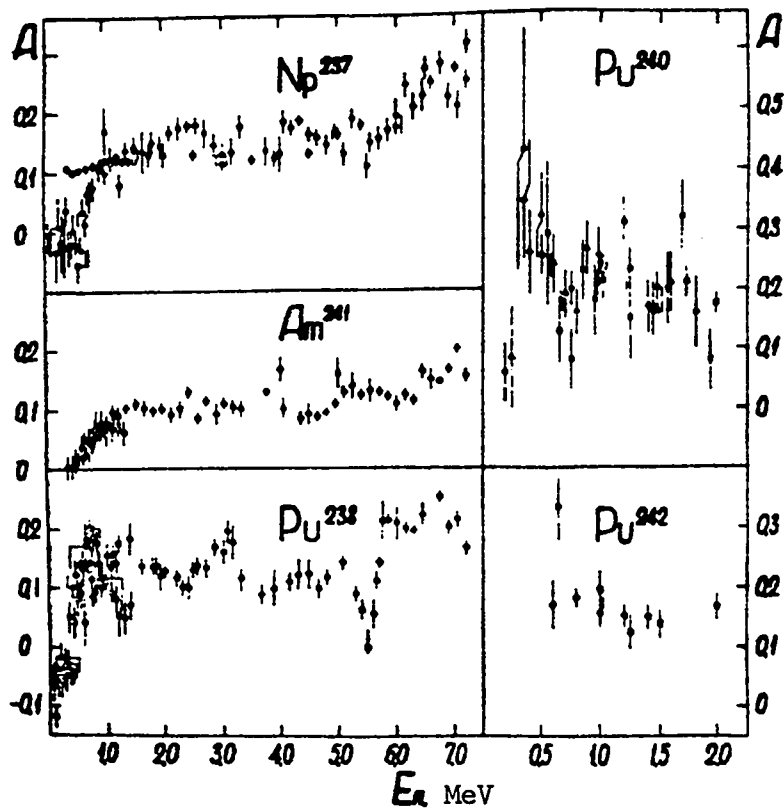


Fig. 4. Coefficient of angular anisotropy of fission as a function of neutron energy for target nuclei  $^{231}\text{Np}$  ( $\circ$  - Ref. 21,  $\blacksquare$  - Ref. 22),  $^{241}\text{Am}$  ( $\circ$  - Ref. 23),  $^{238}\text{Pu}$  ( $\circ$  - Ref. 24),  $^{240}\text{Pu}$  ( $\blacksquare$  - Ref. 26,  $\square$  - Ref. 25,  $\triangle$  - Ref. 8), and  $^{242}\text{Pu}$  ( $\blacksquare$  - Ref. 26). For all nuclei,  $\bullet$  - data of this paper.

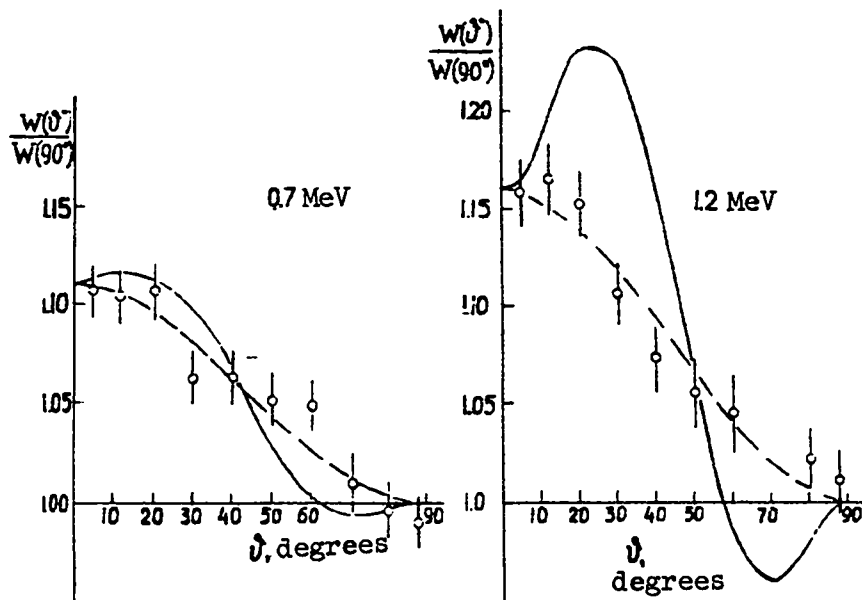


Fig. 5. Angular distributions of fragments during fission of  $^{238}\text{Pu}$  by neutrons;  $\circ$  - 9, curves - calculation (see text).

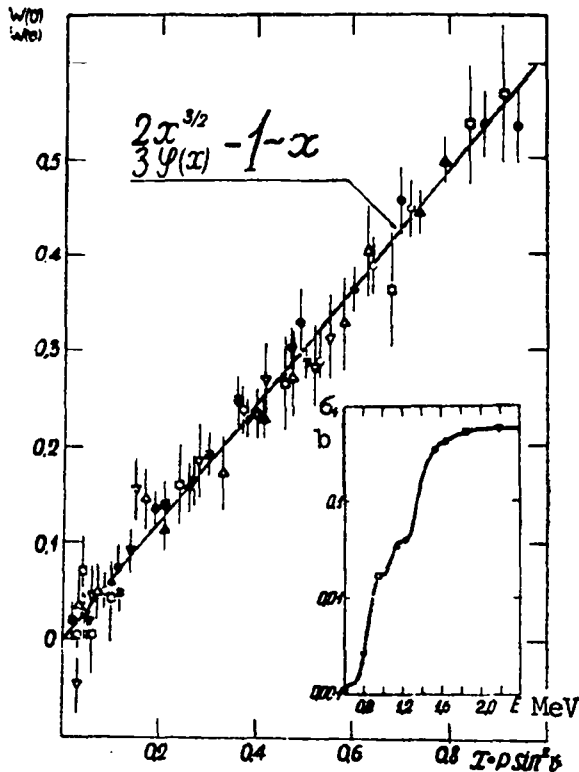


Fig. 6. Comparison of experimental data on  $W(\theta)$  for  $^{238}\text{U}$  with Eq. (5) of the statistical theory of angular distributions of the fission fragments (see text). Insert: energy dependence of the cross section of fission  $\sigma_f(E_k)$  for  $^{238}\text{U}$  by neutrons. Designations:  $\circ$  - 1.25 MeV,  $\bullet$  - 1.55 MeV,  $\blacktriangle$  - 1.65 MeV,  $\nabla$  - 0.8 MeV,  $\square$  - 0.95 MeV,  $\triangle$  - 1.15 MeV,  $\blacksquare$  - 1.85 MeV,  $\blacktriangledown$  - 2.2 MeV.

the hypothesis of Eq. (4), one must use Eq. (5). The most interesting part of the experimental data is summarized in Fig. 6, using

$$\frac{W(0^\circ)}{W(\theta)} = \frac{2}{3} \frac{(p \sin^2 \theta)^{3/2}}{\psi(p \sin^2 \theta)}, \quad (6)$$

which, according to Britt et al.,<sup>5</sup> depends on the single parameter  $X = p \sin^2 \theta$ . The right-hand part of Eq. (6), as is shown in Fig. 6, for  $P \lesssim 1$  depends linearly on  $X$  with good agreement. Thus, fission of  $^{238}\text{U}$  ( $n, f$ ) 0.5 to 0.7 MeV below the threshold occurs as if a significant number of channels took part in it.

The sharp change in character and energy dependence of the angular distribution of fragments

with a small increase of nucleons in the region where the properties of equilibrium nuclei change little is surprising. The A. Bohr model<sup>1</sup> imposes no limitations of  $A$  and  $Z$  on the realization of channel effects for nuclei with the same parity of number of nucleons.

Also interesting is the nonmonotonic energy dependence of the angular anisotropy for significant excitations, where the correct statistical description is certain. The energy-dependent  $K_0^2(E^*)$ , determined from the data on the angular anisotropy in Fig. 4, for compound nuclei, odd-odd  $^{238}\text{Np}$  and odd  $^{239}\text{Pu}$ , are compared in Fig. 7 with the analogous dependence for the even-even nucleus  $^{240}\text{Pu}$ , fissioning in the reactions  $^{239}\text{Pu}(d, pf)^{4,5}$  and  $^{239}\text{Pu}(n, f)^{28,29}$ . The excitation energy in the first two cases was calculated as the difference  $E_n - E_{nf}$ , where  $E_{nf}$  is the neutron energy at which the threshold in the fission cross section is observed.

The presence of a staggered structure in the path of  $K_0^2(E^*)$  for  $^{240}\text{Pu}$  has been interpreted in Ref. 4 and a number of subsequent papers<sup>5,29</sup> as the consequence of a pairing energy gap  $2\Delta_p$  in the spectrum of internal excitations. Using the estimate of the jump  $K_0^2$ ,

$$\delta K_0^2 = 2 \langle K_p^2 \rangle = \frac{N(N+1)}{3} \approx 20, \quad (7)$$

associated with the rupture of a pair of nucleons, Britt et al.<sup>4</sup> obtained  $\Delta_p \approx 1.3$  MeV for the transition state, exceeding by almost a factor of two the equilibrium value  $\Delta_0 \approx 0.7$  MeV. In Eq. (7)  $\langle K_p^2 \rangle$ , equal to  $K_0^2$  for one unpaired particle, was estimated as the average over all the single-particle levels of the last unfilled shell with a total quantum number  $N = 7$  to 8. Analysis of the energy dependence  $K_0^2(E^*)$  in a wider region of excitations up to 30 MeV led Griffin<sup>28</sup> to conclude that the critical energy,  $E_{\text{crit}}^*$ , of the phase transition from a superconducting state to a Fermi-gas state is about 19 MeV, which also corresponds to the anomalously high value  $\Delta_p \approx 1.2$  MeV.

Subsequently, the interpretation of the staggered shape of the dependence  $K_0^2(E^*)$  for low excitations and the reliability of the determination of  $\Delta_p$ ,  $E_{\text{crit}}^*$ , and  $\langle K_p^2 \rangle$  became suspect.<sup>30,31</sup> A re-

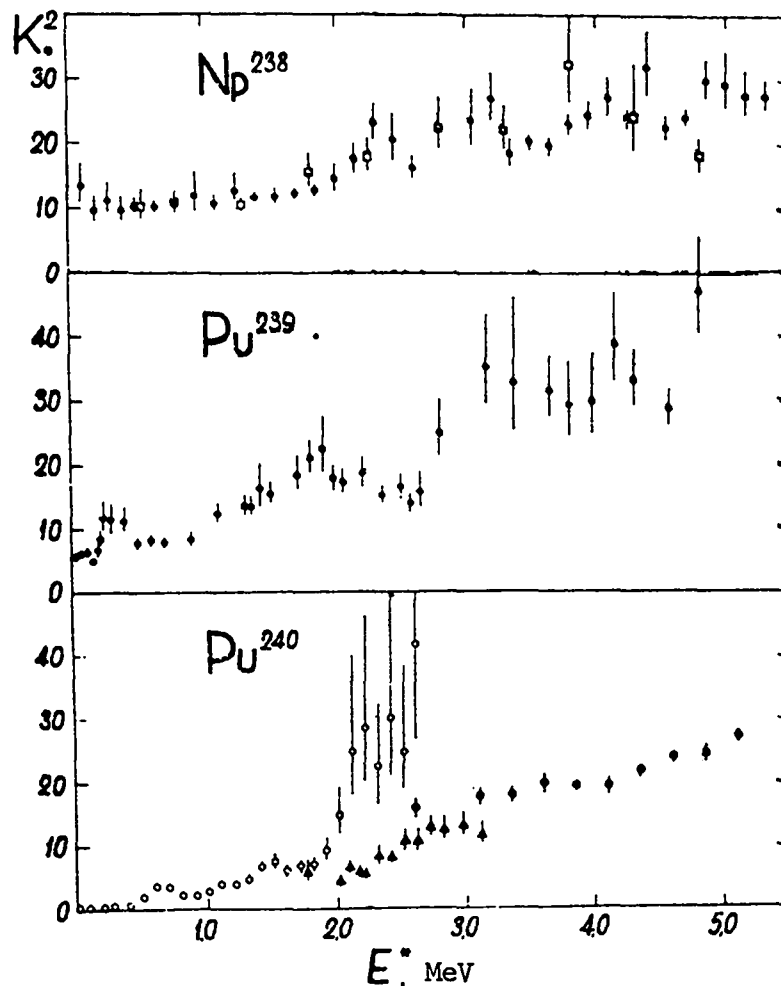


Fig. 7. Dependence of parameter  $K_0^2$  on excitation energy  $E^*$  for fissioning nuclei  $^{238}\text{Np}$ ,  $^{239}\text{Pu}$ , and  $^{240}\text{Pu}$ . On lower drawing:  $\circ$  - Ref. 5,  $\square$  - Ref. 28,  $\blacktriangle$  - Ref. 29.

view of Griffin's analysis<sup>28</sup> led Smirenkin et al.<sup>31</sup> to the considerably lower values,  $E^*_{\text{crit}} = 9.5 \pm 3$  MeV and  $\Delta_f = 0.77 \pm 0.15$  MeV, close to the equilibrium value.  $K_0^2$ , as follows from Fig. 7, for  $E^* \rightarrow 0$  ( $^{238}\text{Np}$  and  $^{239}\text{Pu}$ ) converges to  $\langle K_P^2 \rangle \approx 5$ , not  $\approx 10$ , as predicted by Eq. (7) (see also Ref. 29). From Fig. 7 we see that a factor of 2 decrease in  $\langle K_P^2 \rangle$  with the significant spread of different data on  $K_0^2$  for  $^{240}\text{Pu}$  leads to a large uncertainty in determination of  $\Delta_f$ . Finally, a staggered structure of  $K_0^2(E^*)$  for  $^{238}\text{Np}$  and  $^{239}\text{Pu}$ , each having a spectrum of transition states without an energy gap, negates the possibility of determining  $\Delta_f$  from the value of the jump  $\delta K_0^2$ , Eq. (7).

Rejection of the hypothesis of an anomalous en-

ergy gap value necessitates reevaluating the physical nature of even-odd differences for fission barriers. In many papers, particularly those devoted to systematization of experimental data on the periods of spontaneous fission and the height of the barriers, the differences in even and odd nuclei are related to the difference in the energy surfaces in the transition and equilibrium states; i.e.,  $\Delta_f - \Delta_0$ . Examples of such systematizations<sup>32</sup> are given in Fig. 8. There the values of  $E_f$  were determined for even-even fissioning nuclei from a channel analysis of the angular anisotropy of the fission in (d,pf) and ( $\gamma$ ,f) reactions<sup>5,10</sup> (see Table I), and for odd and odd-odd nuclei, from the threshold observed in the cross sections of fission by neutrons.

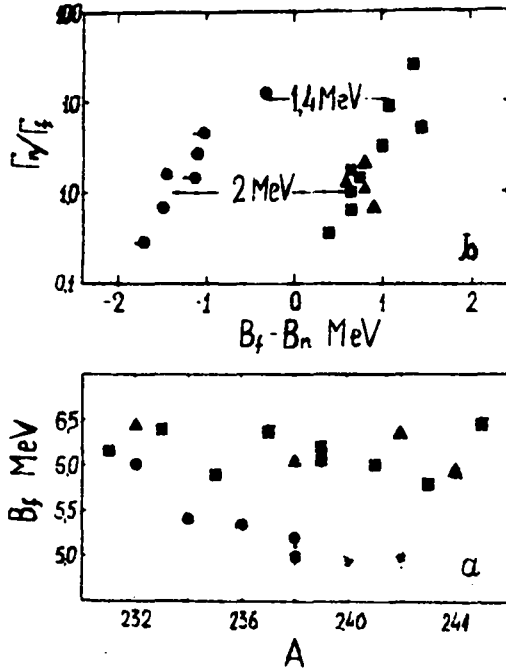


Fig. 8. a) Thresholds of excited fission of even-even ( $\bullet$ ), odd ( $\blacksquare$ ), and odd-odd ( $\blacktriangle$ ) nuclei. b) Ratio of average neutron and fission widths  $\Gamma_n/\Gamma_f$  as a function of the difference  $E_f - B_n$ . Designations are the same as for a).

with deformation of the nucleus, but remains open if one assumes that  $\Delta_f \approx \Delta_0$ .

C. Photofission of the Even-Even Nuclei  $^{232}\text{Th}$ ,  $^{238}\text{U}$ ,  $^{238}\text{Pu}$ ,  $^{240}\text{Pu}$ , and  $^{242}\text{Pu}$ .

Measurements were carried out on the internal tungsten target of a high-current microtron in the range of limiting energies of the bremsstrahlung spectrum of  $\gamma$ -quanta of  $E_{\max} = 5$  to 8 MeV. With excitation by photons of these energies, even-even nuclei are formed only in the  $T^\pi = 1^-$  and  $2^+$  states, as a result of dipole and quadrupole absorption, respectively. The total angular distribution of the fragments, therefore, usually has the form

$$W(\theta) = \alpha + \beta \sin^2 \theta + c \sin^2 2\theta. \quad (8)$$

If, according to A. Bohr's hypothesis,<sup>1</sup> the fission thresholds for the  $T^\pi, K$  states satisfy the relations  $E_f(1^-, 1) > E_f(1^-, 0) > E_f(2^+, 0)$ , then qualitatively the energy dependence of the angular distributions of the fragments must reduce to the ratios

$$b/a = \frac{P(1^-, 0) - P(1^-, 1)}{P(1^-, 1)} \quad \text{and} \quad c/b \approx \frac{3}{4} \frac{\sigma_Y^{2^+}}{\sigma_Y^{1^-}} \frac{P(2^+, 0)}{P(1^-, 0)}, \quad (9)$$

The distance between the two branches of the dependence of  $\Gamma_n/\Gamma_f$  on  $(E_f - B_n)$  can be estimated statistically as  $\Delta_f + \Delta_0$ . According to Fig. 8b it is  $\sim 2$  MeV. Both this value and the splitting of  $E_f$  shown in Fig. 8a correspond to assumption of a significant difference  $\Delta_f - \Delta_0$ , of 0.5 to 0.7 MeV on the average. However, this wide-spread explanation of even-odd differences in  $E_f$  is contradictory, because, using the hypothesis of a significant difference in  $\Delta_f$  and  $\Delta_0$ , one would have to observe a  $\Delta_f - \Delta_0$  splitting in the data of Figs. 8a and 8b for odd and odd-odd nuclei, and this split does not occur (see Ref. 32).

Thus, the question of the nature of even-odd differences in the fission barrier cannot be solved by the hypothesis of increase in the energy gap

which increase with decreasing excitation energy. This corresponds to observation (Fig. 9). For high energies, both ratios are small, because  $P(1^-, 0) - P(1^-, 1) \ll P(1^-, 1)$  and  $\sigma_Y^{2^+}/\sigma_Y^{1^-} \ll 1$ , but in the subbarrier region  $b/a$  reaches 100 ( $^{232}\text{Th}$ ,  $E_{\max} = 5.4$  MeV), and  $c/b \gtrsim 3$  ( $^{240}\text{Pu}$ ,  $E_{\max} = 5$  MeV).

However, a qualitative explanation is difficult. The ratio of penetrabilities of two barriers of different height and peak curvature usually depends monotonically on the energy and has a maximum at the energy coinciding with the peak of the lower barrier. The total photofission cross section near the threshold,  $\sigma_f \approx \sigma_Y^{1^-} \frac{P(1^-, 0)}{P(1^-, 0) + P_c}$ , below the neutron binding energy where

TABLE I  
PARAMETERS OF THE FISSION BARRIER FROM DATA ON THE  $(\gamma, f)$  REACTION

Nucleus	$E_{fB}^{2+,0}$ (MeV)	$E_{fB}^{1-,0}$ (MeV)	$T_f (\approx E_{fA}^{1-,0})$ (MeV)	$\delta AB$ (MeV)
$^{232}\text{Th}$	5.7	6.0	6.0	0*
$^{238}\text{U}$	< 5.0	5.4	5.8	0.4
$^{238}\text{Pu}$	< 5.2	5.4	6.1	0.7
$^{240}\text{Pu}$	< 5.0	5.1	6.0	0.9
$^{242}\text{Pu}$	< 5.0	5.2	6.1	0.9

\* The values of the characteristic given should be considered estimates with an accuracy of  $\sim 0.2$  MeV.

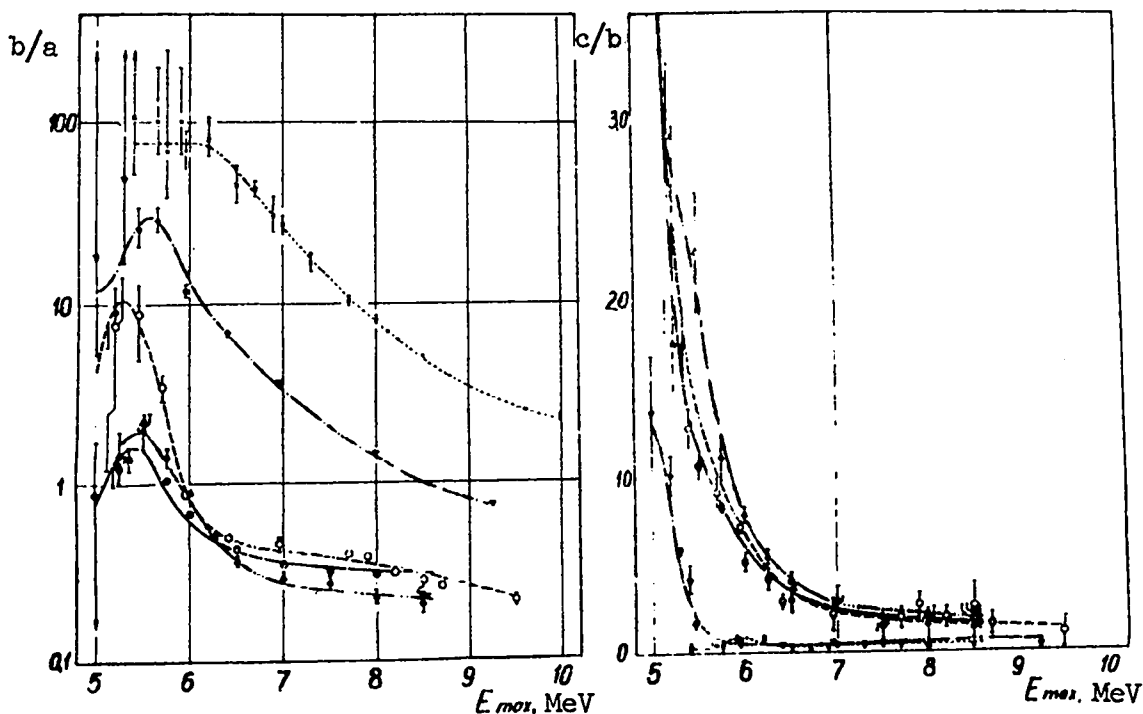


Fig. 9. Ratios of coefficients  $b/a$  and  $c/b$  as a function of  $E_{max}$   
( $\times$  - for  $^{232}\text{Th}$ ;  $\nabla$  - for  $^{238}\text{U}$ ;  $\Delta$  - for  $^{238}\text{Pu}$ ;  
 $\circ$  - for  $^{240}\text{Pu}$ ;  $\bullet$  - for  $^{242}\text{Pu}$ ).

$P_c = \frac{2\pi f \gamma}{D} \ll 1$ , must be equalized with the photofission cross section  $\sigma_\gamma$  and emerge into a plateau for  $P(1^-,1) \ll P(1^-,0) \approx P_c \ll 1$ , i.e., for the energy of the observed threshold  $T_f$ , which is somewhat lower than  $E_f(1^-,0)$ .<sup>33</sup> This is shown schematically in Fig. 10a.

At the top of Fig. 11 we show the direct experimental results in the form of a dependence of the fragment yields  $Y_i (\sum Y_i = Y)$  corresponding to the different components in the angular distribution, Eq. (8), on the limiting energy of the bremsstrahlung spectrum. Using this curve, we determined the energy dependences of the partial components of the photofission cross sections  $\sigma_{fi} (\sum \sigma_{fi} = \sigma_f)$  by conversion to monochromatic  $\gamma$ -quanta (Fig. 11, middle). The corresponding energy dependences of  $b/a$ ,  $c/b$ , and  $\sigma_f$  are given at the bottom of Fig. 11.

The following fact is paradoxical considering the simple concepts just stated: the energy at which anisotropy, the ratio  $b/a$ , is greatest for plutonium isotopes is almost 1 MeV below the observed threshold  $T_f$ , whereas according to the generally accepted description this point must be higher than  $T_f$  (Fig. 10a). Quantitatively, the divergence is very sharp: where  $b/a$  is greatest, the photofission cross section must approximately coincide with its values at the plateau and  $\sigma_\gamma^1$ , but, in fact, it is a hundred times less. When data only on the yields  $Y_i$  and  $b/a$  and  $c/b$  are con-

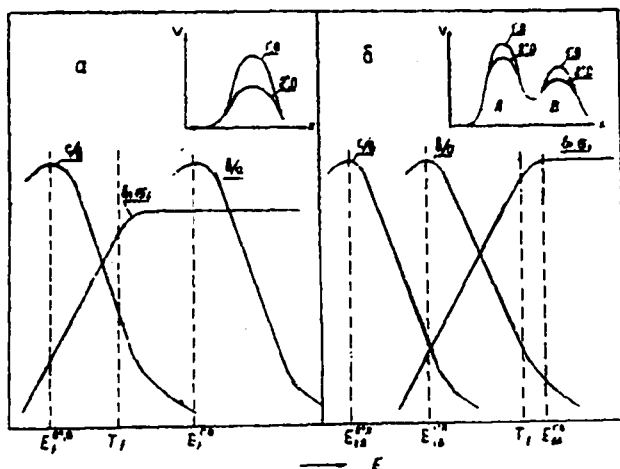


Fig. 10. Dependences of anisotropy and photofission cross section for single - (a) and double-humped (b) barriers depicted schematically.

sidered as a function of  $E_{\max}$ , this fact is not so obvious, but we noted it earlier as difficult to explain by traditional representations, and offered two hypotheses,<sup>3,34</sup> in accordance with which the threshold observed in the angular anisotropy  $E_f^{1-} \sim T_f$ , and not greater than  $T_f$ . However differentiation of  $Y_i(E_{\max})$  showed that this threshold is less than  $T_f$ , and the difference exceeds the limits of any uncertainties.

## II. INTERPRETATION

The important results of the interpretation of the experimental data are as follows.

A. In the energy dependence of the penetrability of the barrier, deviations from an exponential monotonic path are seen in the form of resonances. The locations of the resonances  $P_{K\pi}$  corresponding to various quantum characteristics  $K^\pi$  do not coincide.

B. With increased nucleons in a narrow region of masses of fissioning nuclei, the channel effects near the threshold observed in the cross section disappear, blending into the subthreshold energy region.

C. A number of arguments arise against the hypothesis of a significant difference in the energy gap in the transition and equilibrium states. However, rejection of this hypothesis does not help explain even-odd differences in the fission barriers.

The scope of phenomena that do not fit the traditional fission picture is significantly wider, and exceeds the framework of problems associated with the angular anisotropy of dispersion of fragments (spontaneously fissioning isomers, grouping of resonances of the cross section of fission by slow neutrons). The two-hump barrier model is very fruitful for explaining them.<sup>12,13</sup> According to Strutinskiĭ and Bjornholm,<sup>12</sup> the transition state in the second well (between maxima A and B) is similar to the usual compound state of a nucleus of equilibrium shape. If there is large probability of dissipation of the energy of the collective movement into nucleon degrees of freedom, the nucleus, before splitting, will twice undergo transition of the internal energy into deformation energy. In this sense, the fission reaction can be considered a two-step process. This qualitatively new property is also a source of the effects considered.

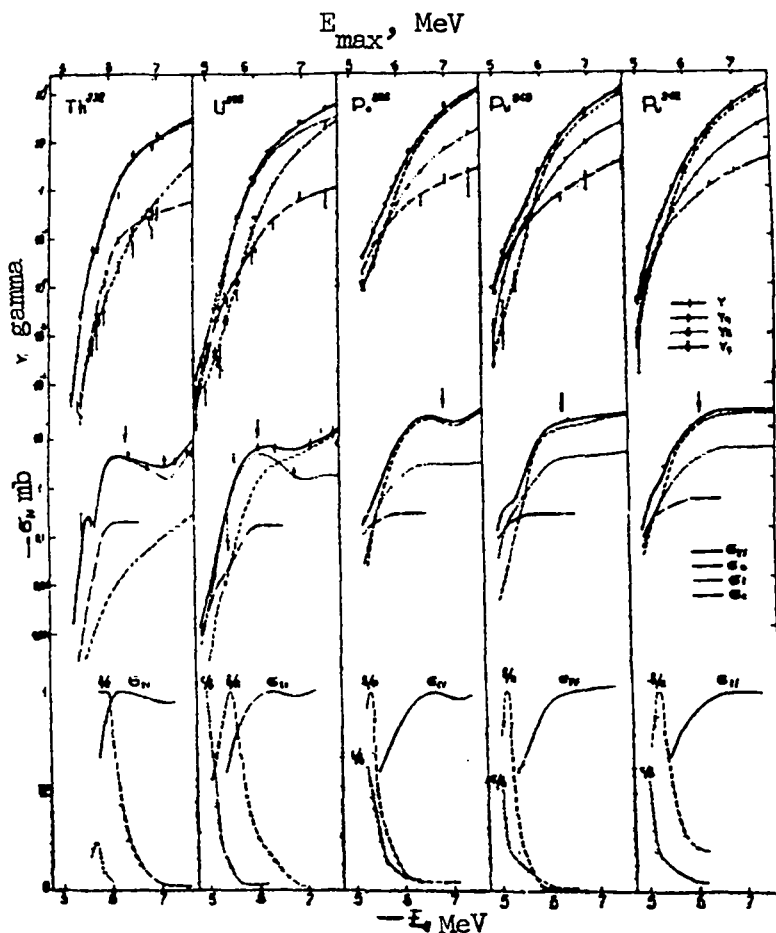


Fig. 11. Energy dependence of yield  $Y(E_{\max})$ , fission cross section  $\sigma_f(E_\gamma)$ , and their angular components  $Y_1(E_{\max})$  and  $\sigma_{f1}(E_\gamma)$  in the  $(\gamma, f)$  reaction.  $E_{\max}$  - limiting energy of bremsstrahlung spectrum,  $E_\gamma$  - energy of monochromatic photons. Above:  $Y(E_{\max})$  and  $Y_1(E_{\max})$ ; middle:  $\sigma_f(E_\gamma)$  and  $\sigma_{f1}(E_\gamma)$ ; below: ratios  $c/b$  and  $b/a$  and  $\ln \sigma_f$  as a function of  $E_\gamma$  in arbitrary units. Vertical arrows show location of neutron binding energy  $B_n$ .

The presence of quasi-stationary levels in the second well leads to a penetrability of the barrier which, unlike the monotonic function, Eq. (2), near the levels is changed by the resonance shape.<sup>12,13</sup> In addition to the  $\sim 0.1$ -MeV-wide resonances of the type realized during the fission of  $^{232}\text{Th}$  by fast neutrons, in the cross section of fission by slow neutrons a grouping of strong and weak resonances is observed--a structure with an envelope resonance width of  $\sim 0.01$  to  $0.1$  keV and  $\sim 0.01$  to  $10$  keV distance between resonances. According to Ref. 12, the first are associated with the vibration states and

the second with the internal excitation states.

Originally, resonances of the first type were attributed to the states in the first well,<sup>7,36</sup> but study of the dissipation of the vibratory energy into internal degrees of freedom led to questioning this possibility.<sup>12,13</sup> In solving this question, apparently, the resonances of the penetrability of a certain  $K^\pi$  combination are very important (see Fig. 3). If the vibratory states are associated with the first well, one has to enlist too strong an assumption of the preservation of  $K$  during the whole evolution of the fissioning nucleus to explain

this fact.

The locations of resonances with different  $K^\pi$  do not reveal a regular structure; the distance between them (Fig. 3) is often significantly less than that expected for vibration states ( $\sim \hbar\omega \approx 0.5$  to 1 MeV). This seems to show that it is logical to attribute  $P_{K^\pi}$  resonances for different  $K^\pi$  combinations to vibration states in different wells. In other words, it indicates a splitting of the curves of the potential energy of deformation as a function of the quantum characteristics, in conformity with A. Bohr's model.<sup>1</sup> The quasi-stationary states in the second well caused by the resonance change in  $P_{K^\pi}(E)$  contribute significantly to development of channel effects in the fission of nuclei.

The disappearance of channel effects in the angular anisotropy of fission near the cross-section threshold when the nucleons in the fissioning nuclei increase, is associated with the structural change in the two-hump barrier, according to Ref. 12, with the decreased maximum B and deepening of the well between the maxima. Let us assume, following Ref. 12, that the well in the barrier is deep enough and that the nucleus in it lives long enough relative to the characteristic period of K migration to "forget" the quantum states it occupied during passage of the first barrier A. Subsequent development of the fission process is determined by the spectrum of states in barrier B.

In the  $E_{FB} \gtrsim E_{FA}$  case, the traditional situation exists: diversity of  $W(\theta)$  shapes and significant change of the angular anisotropy near the observed fission threshold. In the opposite case,  $E_{FB} < E_{FA}$ , a new situation can arise because the threshold observed in the cross section is determined by the height of the larger of the barriers,  $E_{FA}$ , and the realized fission-channel spectrum is determined by the excitation energy at the critical point, B. For a sufficient difference,  $\delta_{AB} = E_{FA} - E_{FB} > 0$ , the channel effects in the angular distributions of the fragments will appear in the essentially subbarrier energy region. Thus, near the threshold the fission-channel density can already be significant, so that there will be a nearly statistical K distribution.

Our experimental determination of the changes in  $W(\theta)$  and  $A(E)$  agrees satisfactorily with this

description. The threshold values obtained by analysis of the experimental photofission data (Fig. 10b and 11) are given in Table I. The lower estimate of  $\delta_{AB} \approx T_f - E_{FB}^{1-,0}$  increases from thorium to plutonium, in conformity with the predictions of Strutinskii and Bjornholm.<sup>12</sup> We assume that the locations of the maxima of  $b/a$  are not related to the quasi-stationary states  $(T^\pi, K) = (1^-, 0)$ , because  $\sigma_b$  runs smoothly near the  $E_{FB}^{1-,0}$  threshold, decreasing exponentially with decreased photon energy. Because  $c/b$  usually increases monotonically with decreasing energy, the upper limiting values in the table are given for the  $E_{FB}^{2+,0}$  threshold.

The values of  $\delta_{AB}$  in Table I agree with the estimates obtained from an analysis of the grouping of resonances of the cross section for fission of  $^{237}\text{Np}$  and  $^{240}\text{Pu}$  by slow neutrons.<sup>35</sup> Note that the displacement of the channel effects in the angular anisotropy into the energy region which is subbarrier with respect to the fission cross section apparently is also observed in investigations of reactions of the  $(d, pf)$  type. Experimental data<sup>4,5</sup> show that the maximum angular anisotropy for which the states  $K = 0$  are responsible is in the  $E < B_n$  region, where the fissionability of the nuclei  $\frac{\sigma_f}{\sigma_c} \approx \frac{\Gamma_f}{\Gamma_\gamma} \ll 1$ . To explain this paradox, Britt et al.,<sup>5</sup> in our opinion, relied too much on the assumption that the radiation width  $\Gamma_\gamma$  is approximately an order of magnitude greater than the values observed for  $E \approx B_n$  in  $(n, \gamma)$  reactions.

Using a two-hump fission barrier model, one can also grasp the nature of the even-odd differences in  $E_f$  presented in Fig. 8. Because the heights of the fission barriers determined from the energy dependences of the angular anisotropy (even-even nuclei) and the fission cross section (odd and odd-odd nuclei) belong to barriers B and A, respectively, one must consider the difference  $\delta_{AB}$  in analysis of even-odd differences of  $E_f$ . The splitting of  $E_f$  shown in Fig. 8a also corresponds to this value, decreasing, as in Table I, to the side of lighter fissioning nuclei. The distance between the branches of the set  $\Gamma_n/\Gamma_f = f(E_f - B_n)$  for heavy nuclei ( $\Gamma_n/\Gamma_f < 1$ ) includes  $\delta_{AB} = 2 \text{ MeV} - (\Delta_f + \Delta_0) \approx 0.6 \text{ MeV}$  for  $\Delta_f \approx \Delta_0 \approx 0.7 \text{ MeV}$ . For light nuclei ( $\Gamma_n/\Gamma_f \gg 1$ ), as shown in Fig. 8b, this distance decreases to  $\Delta_f + \Delta_0 \approx 1.4 \text{ MeV}$ , agreeing with  $\delta_{AB} \approx 0$ .



Let us note, in conclusion, one more consequence of the description of fission probability as a whole. The properties of the angular distributions of fragments show that in addition to the channel effects associated with quasi-stationary states in the second well, channel effects in the old sense, i.e., those caused by the splitting of the states in barrier B, are realized in the fission. In this, it is logical to count the number of channels determining the probability of fission from barrier B, and not from the bottom of the second well, as could be expected from the role of quasi-stationary states. The given hypothesis confirms the value of  $K_0^2$  for energies near the threshold:  $K_0^2$  for even-even nuclei, according to the degree of approach to barrier B, converges to zero, and for odd nuclei, to the single-particle value (Fig. 7). An example of the calculation of the cross section of fission of  $^{240}\text{Pu}$  by fast neutrons with this hypothesis, that satisfactorily describes the experimental data in the near-threshold energy region, is given by Gai et al.<sup>35</sup>

We thank P. L. Kapitsa, A. I. Leipunskii, and V. M. Strutinskii for their interest in the investigations, and M. K. Golubeva and N. E. Fedorova for their work in scanning the glass detectors widely used in the measurements.

### III. REFERENCES

1. A. Bohr, Int. Conf. Peaceful Uses At. Energy, Geneva, 1955, Proceedings, Vol. 2, p. 151.
2. J. A. Wheeler, Fast Neutron Physics, Part II, J. B. Marlon and J. L. Fowler, Eds., Interscience, New York, 1963, Vol. II, p. 2051.
3. N. S. Rabotnov, G. N. Smirenkin, A. S. Soldatov, L. N. Usachev, S. P. Kapitsa and Iu. M. Tsipeniuk, "Physics and Chemistry of Fission," Symp. Phys. Chem. Fission, Salzburg, 1965, Proceedings, Vol. 1, p. 135, IAEA, Vienna (1965).
4. H. C. Britt, W. R. Gibbs, J. J. Griffin, and R. H. Stokes. Phys. Rev. Letters 11, 343, (1963); Phys. Rev. 139, B354 (1965)
5. H. C. Britt, F. A. Rickey, Jr., and W. S. Hall, Rep. LA-DC-9562, 1968. (Note: published in Physical Review 175, 1525 (1968).
6. P. E. Vorotnikov, S. M. Dubrovina, G. A. Otroshchenko, and V. A. Shigin, Yadern. Fiz. 2, 295 (1967); P. E. Vorotnikov and G. A. Otroshchenko, Yadern. Fiz. 7, 1228 (1968).
7. J. E. Lynn, "Nuclear Data for Reactors," Proc. Symp. Paris, Vol. II, p. 89, IAEA, Vienna, 1967.
8. R. W. Lamphere, "Physics and Chemistry of Fission," Proc. Symp. Phys. Chem. Fission, Salzburg, 1965, Vol. 1, p. 63.
9. K. D. Androsenko and G. N. Smirenkin, Pis'ma ZhETF, 8, 181 (1968); D. L. Shpak and G. N. Smirenkin, Pis'ma ZhETF 8, 545 (1968); 2, 196 (1969).
10. S. P. Kapitsa, N. S. Rabotnov, G. N. Smirenkin, A. S. Soldatov, L. N. Usachev, and Iu. M. Tsipeniuk, Pis'ma ZhETF 2, 128 (1969).
11. V. M. Strutinskii, Nucl. Phys. A95, 420 (1967).
12. V. M. Strutinskii and S. Bjornholm, Int. Symp. Nucl. Structure, Dubna, 1968.
13. J. E. Lynn, Int. Symp. Nucl. Structure, Dubna, 1968.
14. S. B. Ermagambetov, V. F. Kuznetsov, and G. N. Smirenkin, Yadern. Fiz. 2, 257 (1967).
15. R. L. Henkel and J. E. Brolley, Jr., Phys. Rev. 103, 1292 (1956); S. Lo Nigro and C. Milone. Nucl. Phys. A96, 617 (1967).
16. A. N. Behkami, J. R. Huizenga, and J. H. Roberts, Nucl. Phys. A118, 65 (1968).
17. S. B. Ermagambetov, V. E. Kolesov, V. G. Nesterov, G. N. Smirenkin, and A. S. Tishin, Yadern. Fiz. 8, 704 (1968).
18. A. N. Behkami, J. H. Roberts, W. Loweland, and J. R. Huizenga, Phys. Rev. 171, 1267 (1968).
19. E. I. Korneev, V. S. Skobkin, and G. N. Florov, Zh. Eksperim. i Teor. Fiz. 37, 41 (1959).
20. J. Pedersen and B. D. Kuzminov, Phys. Letters 29B, 176 (1969).
21. B. M. Gokhberg, G. A. Otroshchenko, and V. A. Shigin, Dokl. Akad. Nauk 128, 1157 (1959).
22. J. E. Simmons and R. L. Henkel, Phys. Rev. 120, 198 (1960).
23. P. E. Vorotnikov, S. M. Dubrovina, G. A. Otroshchenko, and V. A. Shigin, Dokl. Akad. Nauk 169, 314 (1966).
24. P. E. Vorotnikov, S. M. Dubrovina, G. A. Otroshchenko, and V. A. Shigin, Yadern. Fiz. 3, 479 (1966).
25. V. G. Nesterov, G. N. Smirenkin, and I. I. Bondarenko, At. Energ. (USSR), 10, 620 (1961).
26. J. E. Simmons, R. B. Perkins, and R. L. Henkel, Phys. Rev. 137, B809 (1965).
27. V. M. Strutinskii, At. Energ. (USSR), 2, 508 (1957).
28. J. J. Griffin, Phys. Rev. 132, 2204 (1963).
29. J. R. Huizenga, A. N. Behkami, J. W. Meadows, Jr., and E. D. Klema, Phys. Rev. 174, 1539 (1968).
30. V. M. Strutinskii and V. A. Pavlinchuk, "Physics and Chemistry of Fission," Proc. Symp. Chem. Fission, Salzburg, 1965, Vol. 1, p. 127, IAEA, Vienna (1965).
31. G. N. Smirenkin, V. G. Nesterov, and A. S. Tishin, Yadern. Fiz. 6, 921 (1967).

32. A. V. Ignatyuk and G. N. Smirenkin, Phys. Letters 29B, 159 (1969).
33. L. N. Usachev, V. A. Pavlinchuk, and N. S. Rabotnov, At. Energ. (USSR) 17, 479 (1964).
34. N. S. Rabotnov, G. N. Smirenkin, A. S. Soldatov, L. N. Usachev, S. P. Kapitza, and J. M. Zipevnyuk, Phys. Letters 26B, 218 (1968).
35. E. Gai, A. V. Ignatiuk, N. S. Rabotnov, and G. N. Smirenkin, 2nd Symp. Phys. Chem. Fission, Vienna, 1969, Paper SM/122/132. Also prepared as FEL-184.
36. B. T. Geilikman, Yadern. Fiz. 9, 535 (1969).